

A Pacific Interdecadal Climate Oscillation with Impacts on Salmon Production*



Nathan J. Mantua,⁺ Steven R. Hare,[#] Yuan Zhang,⁺
John M. Wallace,⁺ and Robert C. Francis[@]

ABSTRACT

Evidence gleaned from the instrumental record of climate data identifies a robust, recurring pattern of ocean-atmosphere climate variability centered over the midlatitude North Pacific basin. Over the past century, the amplitude of this climate pattern has varied irregularly at interannual-to-interdecadal timescales. There is evidence of reversals in the prevailing polarity of the oscillation occurring around 1925, 1947, and 1977; the last two reversals correspond to dramatic shifts in salmon production regimes in the North Pacific Ocean. This climate pattern also affects coastal sea and continental surface air temperatures, as well as streamflow in major west coast river systems, from Alaska to California.

September 1915 (*Pacific Fisherman* 1915)

Never before have the Bristol Bay [Alaska] salmon packers returned to port after the season's operations so early.

The spring [chinook salmon] fishing season on the Columbia River [Washington and Oregon] closed at noon on August 25, and proved to be one of the best for some years.

1939 Yearbook (*Pacific Fisherman* 1939)

The Bristol Bay [Alaska] Red [sockeye salmon] run was regarded as the greatest in history.

The [May, June and July chinook] catch this year is one of the lowest in the history of the Columbia [Washington and Oregon].

August/September 1972 (*National Fisherman* 1972)

Bristol Bay [Alaska] salmon run a disaster.

Gillnetters in the Lower Columbia [Washington and Oregon] received an unexpected bonus when the largest run of spring chinook since counting began in 1938 entered the river.

1995 Yearbook (*Pacific Fishing* 1995)

Alaska set a new record for its salmon harvest in 1994, breaking the record set the year before.

Columbia [Washington and Oregon] spring chinook fishery shut down; west coast troll coho fishing banned.

*JISAO Contribution Number 379.

⁺Joint Institute for the Study of the Atmosphere and Oceans, University of Washington, Seattle, Washington.

[#]International Pacific Halibut Commission, University of Washington, Seattle, Washington.

[@]Fisheries Research Institute, University of Washington, Seattle, Washington.

Corresponding author address: Nathan Mantua, Joint Institute for the Study of the Atmosphere and Oceans, University of Washington, Box 354235, Seattle, WA 98195-4235.

E-mail: mantua@atmos.washington.edu.

In final form 6 January 1997.

1. Introduction

Pacific salmon production has a rich history of confounding expectations. For much of the past

two decades, salmon fishers in Alaska have prospered while those in the Pacific Northwest have suffered. Yet, in the 1960s and early 1970s, their fortunes were essentially reversed. Could this pattern of alternating fishery production extremes be connected to climate changes in the Pacific basin?

In this article we present a synthesis of results derived from the analyses of climate records and data describing biological aspects of variability in the large marine ecosystems of the northeast Pacific Ocean. Our goal is to highlight the widespread connections between interdecadal climate fluctuations and ecological variability in and around the North Pacific basin.

A considerable body of literature has been devoted to the discussion of persistent widespread changes in Pacific basin climate that took place in the late 1970s (Namias 1978; Trenberth 1990; Ebbesmeyer et al. 1991; Graham 1994; Trenberth and Hurrell 1994). Several studies have also documented interdecadal climate fluctuations in the Pacific basin, of which the changes that took place in the late 1970s are but a single realization (Ebbesmeyer et al. 1989; Francis and Hare 1994 and Hare and Francis 1995, hereafter FH-HF; Latif and Barnett 1994, 1996; Ware 1995; Hare 1996; Zhang 1996; Zhang et al. 1997, hereafter ZWB).

Widespread ecological changes related to interdecadal climate variations in the Pacific have also been noted. Dramatic shifts in an array of marine and terrestrial ecological variables in western North America coincided with the changes in the state of the physical environment in the late 1970s (Venrick et al. 1987; Ebbesmeyer et al. 1991; Brodeur and Ware 1992; Roemmich and McGowan 1995; Francis et al. 1997). Rapid changes in the production levels of major Alaskan commercial fish stocks have been connected to interdecadal climate variability in the northeast Pacific (Beamish and Boullion 1993; Hollowed and Wooster 1992; FH-HF), and similar climate–salmon production relationships have been observed for some salmon populations in Washington, Oregon, and California (Francis and Sibley 1991; J. Anderson 1996, personal communication).

Our results add support to those of previous studies suggesting that the climatic regime shift of the late 1970s is not unique in the century-long instrumental climate record, nor in the record of North Pacific salmon production. In fact, we find that signatures of a recurring pattern of interdecadal cli-

mate variability are widespread and detectable in a variety of Pacific basin climate and ecological systems. This climate pattern, hereafter referred to as the Pacific (inter) Decadal Oscillation, or PDO (following coauthor S.R.H.'s suggestion), is a pan-Pacific phenomenon that also includes interdecadal climate variability in the tropical Pacific.

2. Data and methodology

We analyze a wide collection of historical records of Pacific basin climate and selected commercial salmon landings. Specifically, this study examines records of (i) tropical and Northern Hemisphere extratropical sea surface temperature (SST) and sea level pressure (SLP); (ii) wintertime North American land surface air temperatures and precipitation; (iii) wintertime Northern Hemisphere 500-mb height fields; (iv) SST along the west coast of North America; (v) selected streamflow records from western North America; and (vi) salmon landings from Alaska, Washington, Oregon, and California.

Monthly mean SST data for the period of record 1900–93 were obtained from an updated version of the quality-controlled U.K. Meteorological Office Historical SST Dataset (HSSTD) provided by the Climatic Research Unit, University of East Anglia (Folland and Parker 1990, 1995). These data are on a 5° lat \times 5° long grid. The monthly mean, 1° lat \times 1° long gridded data of the Optimally Interpolated SST (OISST, Reynolds and Smith 1995) are averaged into 5° boxes and used to extend the HSSTD through the January 1994–May 1996 period of record. We also use 2° lat \times 2° long Comprehensive Ocean–Atmosphere Data Set (COADS, Fletcher et al. 1983) SST for the period of record 1900–92 in the construction of Fig. 2.

Monthly mean SLP data were obtained from two sources: first, 5° lat \times 5° long gridded fields from the Data Support Section/Computing Facility at the National Center for Atmospheric Research (NCAR) for the period of record 1900–May 1996 (Trenberth and Paolino 1980); and second, 2° lat \times 2° long gridded surface marine observations from COADS for the period of record 1900–92, which are used to construct the station-based Southern Oscillation Index (SOI) shown in Fig. 1 and the SLP map in Fig. 2.

For the period of record 1900–92, the COADS-based SOI used here was constructed following

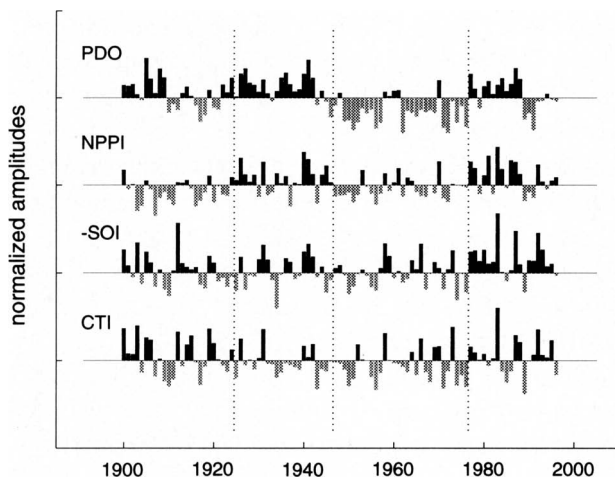
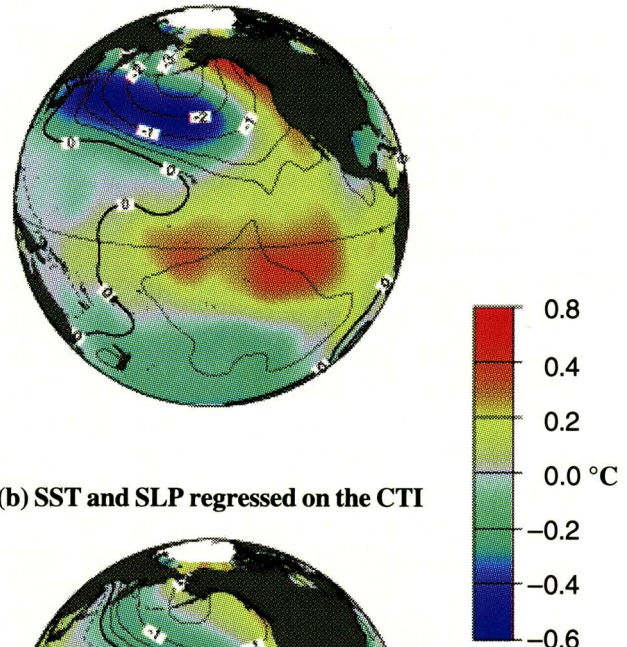


FIG. 1. Normalized winter mean (November–March) time histories of Pacific climate indices. Dotted vertical lines are drawn to mark the PDO polarity reversal times in 1925, 1947, and 1977. Positive (negative) values of the NPPI correspond to years with a deepened (weakened) Aleutian low. The negative SOI is plotted so that it is in phase with the tropical SST variability captured by the CTI. Positive value bars are black, negative are gray.

ZWB. The Tahiti pole is defined as the average SLP anomaly from 20°N to 20°S latitude from the international date line to the coast of South and Central America, while the Darwin pole is defined as the average SLP anomaly over the remainder of the global tropical oceans within the same range of latitudes. Missing SOI values for the period of record 1913–20 and 1993–May 1996, were estimated from a linear regression with the traditional Tahiti–Darwin SOI based on the common period of record 1933–90, obtained from the National Oceanic and Atmospheric Administration/National Centers for Environmental Prediction (NOAA/NCEP) Climate Prediction Center. For an early description of the Southern Oscillation the reader is referred to Walker and Bliss (1932).

Gridded, global, land surface air temperature and precipitation anomalies for the period of record 1900–92, based on station data, were obtained from the Carbon Dioxide Information Analysis Center in Oak Ridge, Tennessee. The air temperature data are provided as monthly anomalies on a 5° lat × 10° long grid, over land only (Jones et al. 1985). We used “cold-season” means (November–March) for Fig. 3a. The precipitation anomalies are provided as (3 month) seasonal mean anomalies on a 4° lat × 5° long grid, over land only (Eischeid et al. 1991). We used the December–February seasonal mean anomalies in constructing Fig. 3b.

(a) SST and SLP regressed on the PDO index



(b) SST and SLP regressed on the CTI

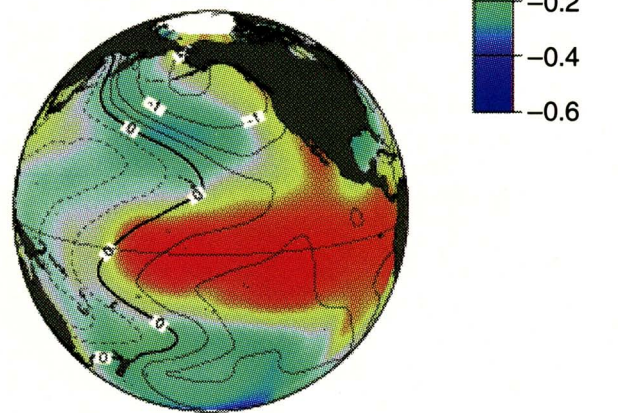


FIG. 2. COADS SST (color shaded) and SLP (contoured) regressed upon (a) the PDO index and (b) the CTI for the period of record 1900–92. Contour interval is 1 mb, with additional contours drawn for ± 0.25 and 0.50 mb. Positive (negative) contours are dashed (solid).

Gridded, Northern Hemisphere 500-mb height fields were obtained from NMC (National Meteorological Center, now NCEP) operational analysis fields, as described by Kushnir and Wallace (1989). November through March mean anomalies were used in constructing Fig. 4.

Monthly mean streamflow records for the Kenai River at Cooper's Landing, Alaska; the Skeena River at Usk, British Columbia, Canada and the Fraser River at Hope, British Columbia, Canada; and the Columbia River at The Dalles, Oregon, were obtained from the National Water Data Exchange, which is part of the United States Geological Survey (USGS). The monthly records were used to generate annual water year (October–September)

flow indices for each stream. The time series labelled BC/Columbia Streamflow in Fig. 5 is a composite of the normalized Skeena, Fraser, and Columbia river water year streamflow anomalies.

Coastal SST time series for British Columbia stations were obtained from the Institute of Ocean Sciences in Sidney, British Columbia, Canada. The time series for coastal BC SST shown in Fig. 5 is a composite of eight individual time series from the following coastal observing stations: Amphitrite Point, Departure Bay, Race Rocks, Langara Island, Kains Island, McInnes Island, Entrance Island, and Pine Island. We use a composite index in an attempt to emphasize regional-scale nearshore SST variability over the finescale variability that exists in that topographically diverse region.

Monthly mean values for Scripps Pier SST were obtained from the Scripps Institution of Oceanog-

raphy in La Jolla, California. Scripps Pier SST variability is well correlated with that along the Alta and Baja California coastline (J. McGowan 1996, personal communication).

Coastal Gulf of Alaska cold season air temperatures were obtained from the National Climate Data Center. The November–March mean Gulf of Alaska air temperatures shown in Fig. 5 are a composite of Kodiak, King Salmon, and Cold Bay, Alaska, station records.

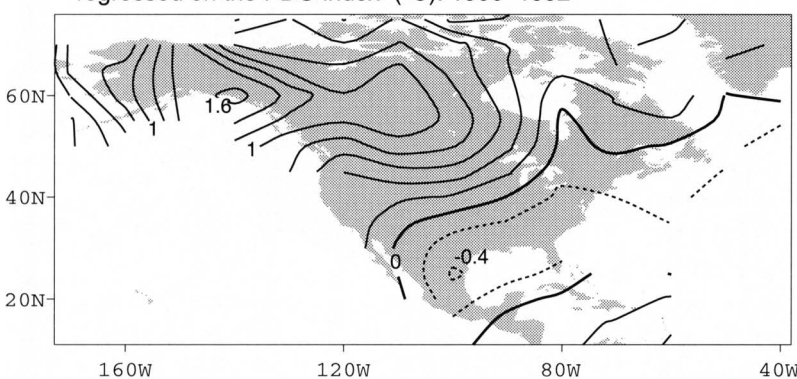
Prior to compositing, each individual SST, streamflow, and air temperature time series was normalized with respect to the 1947–95 period of record, a period for which data are available for all the time series used in the construction of Fig. 5. The mean for the available period of record was then removed from the composite time series before plotting in Fig. 5.

Alaska salmon landings for the period of record 1925–91 were provided by the Alaska Department of Fish and Game (1991). Catch data for 1992 through 1995 were obtained from Pacific Fishing magazine (1994, 1995). We focus on the catch records of sockeye salmon in western and central Alaska, and that of pink salmon in central and southeast Alaska (shown in Fig. 6). These four regional stocks account for about 75% of Alaska's annual salmon catch. The period of record from 1920 through the 1930s represents a "fishing-up" period while the industry was experiencing rapid growth. Subsequent to the late 1930s, fisheries for these stocks have been fully developed, and the catch records are good indicators of stock abundance (Beamish and Bouillon 1993; FH–HF).

Additionally, the record of chinook salmon catch from the Columbia River for the period of record 1938–93 and coho landings from Washington–Oregon–California (WOC) for the period of record 1925–93 are also shown. These records were obtained from the Washington Department of Fisheries (WDF), the Oregon Department of Fish and

(a) Nov–Mar surface air temperature

regressed on the PDO index ($^{\circ}\text{C}$): 1900–1992



(b) Dec–Feb precipitation correlations

with the PDO index ($\times 100$): 1900–1992

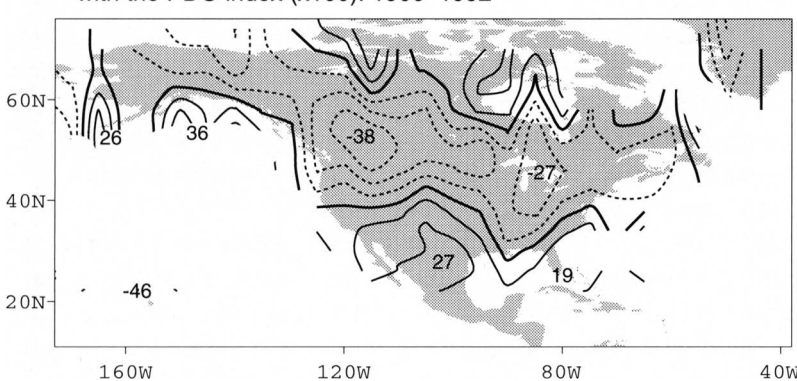


FIG. 3. Maps of PDO regression and correlation coefficients: (a) November–March surface air temperature regressed upon the PDO index shown in Fig. 1; contour interval is 0.2°C . (b) Correlation coefficients ($\times 100$) between December–February precipitation and the PDO index shown in Fig. 1; contour interval is 10. Positive (negative) contours are solid (dashed).

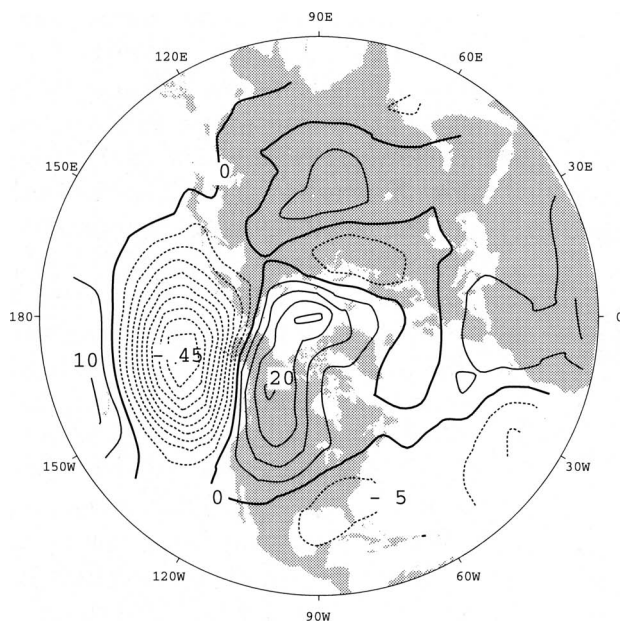


FIG. 4. Wintertime Northern Hemisphere 500-mb heights regressed upon the PDO index for the period of record 1951–90. Contour interval is 5 m, positive (negative) contours are solid (dashed).

Wildlife (ODFW), and the California Department of Fish and Game (WDF and ODFW 1992).

Parallel EOF/PC analyses of the monthly SST and SLP anomaly fields, carried out independently by two of the present authors, were based on the temporal covariance matrix from the 1900–93 period of record. For SST, we used the covariance matrix created from monthly HSSTD anomalies poleward of 20°N in the Pacific basin (Zhang 1996). For SLP, we used the covariance matrix created from monthly NCAR SLP anomalies poleward of 20°N and between 110°E and 110°W (Hare 1996). The resulting November–March mean PCs were normalized prior to plotting in Fig. 1. The leading PC for SLP in the North Pacific sector is labelled NPPI, while that for SST is labelled PDO.

3. Characteristics of the PDO

Of particular interest to this study is the fact that, since at least the 1920s, interdecadal fluctuations in the dominant pattern of North Pacific SLP (NPPI) have closely paralleled those in the leading North Pacific SST pattern (PDO) (Fig. 1; Zhang 1996; ZWB; Latif and Barnett 1996). It is this coherent, interdecadal timescale ocean–atmosphere covari-

ability that we see as the essence of the PDO climate signature. For convenience, throughout the remainder of this report we refer to the time history of the leading eigenvector of North Pacific SST as an index for the state of the PDO.

Also shown in Fig. 1 are the SOI and the Cold Tongue Index (CTI, which is the average SST anomaly from 6°N to 6°S, 180° to 90°W), indices commonly used to monitor the atmospheric and oceanic aspects of ENSO, respectively. The SOI and CTI are correlated with the PDO (see Table 1) such that warm- (cold-) phase ENSO-like conditions tend to coincide with the years of positive (negative) polarity in the PDO. Interestingly, fluctuations in the CTI are mostly interannual, while those in the PDO are predominantly interdecadal (ZWB).

Interdecadal and interannual timescales are both apparent in the indices of atmospheric variability at low and high northern latitudes over the Pacific. The NPPI and SOI are correlated such that the mean wintertime Aleutian Low tends to be more (less) intense during winters with weakened (intensified) easterly winds near the equator in the Pacific.

Correlations between the atmospheric and oceanic climate indices shown in Fig. 1 within respective high- and low-latitude ranges are relatively strong. The NPPI is moderately well correlated with that of the extratropical SST, while at tropical latitudes the SOI and CTI are very well correlated (see Table 1).

By regressing the records of wintertime SST and SLP upon the PDO index, the spatial patterns typically associated with a positive unit standard deviation of the PDO are generated (Fig. 2a). The largest PDO-related SST anomalies are found in the

TABLE 1. Correlation coefficients for the Pacific basin climate indices, shown in Fig. 1, for the period of record 1900–92. Correlation coefficients have been adjusted to reflect the effective degrees of freedom, as a function of autocorrelation, in each time series.

	PDO	NPPI	SOI	CTI
PDO	—	0.50	-0.35	0.38
NPPI	—	—	-0.39	0.42
SOI	—	—	—	-0.82
CTI	—	—	—	—

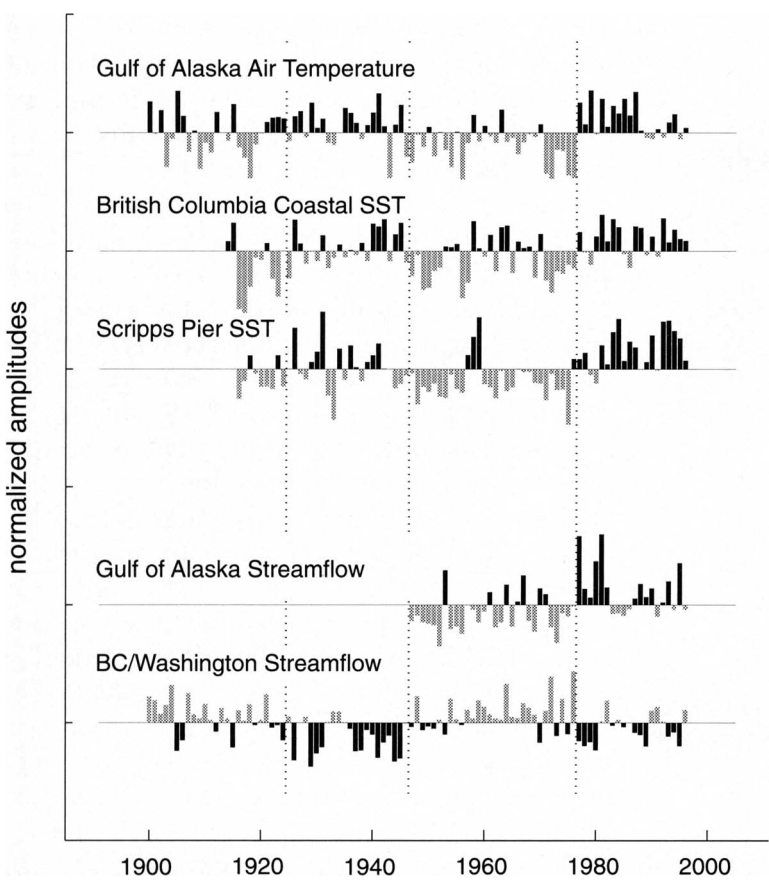


FIG. 5. Selected regional climate time series with PDO signatures. Dotted vertical lines are drawn to mark the PDO polarity reversal times in 1925, 1947, and 1977. Bars are shaded as in Fig. 1, with the shading convention reversed for the BC/Washington streamflow index.

central North Pacific Ocean, where a large pool of cooler than average surface water has been centered for much of the past 20 yr. The peak amplitude of the SST regression coefficients in the cold pool are on the order of -0.5°C . The narrow belt of warmer than average SST that, in the past two decades, has prevailed in the nearshore waters along the west coast of the Americas is also a distinctive feature of this pattern. Note also that the Southern Hemisphere midlatitude SST signature is very similar to that in the northern extratropics. The SLP anomalies that are typical of the positive PDO are characterized by basin-scale negative anomalies between 20° and 60°N . The peak amplitude of the midlatitude wintertime SLP signature is about 4 mb, which represents an intensification of the climatological mean Aleutian low. This SLP pattern is very similar to the dominant pattern of wintertime North Pacific SLP variability. It is noteworthy that there are no strong PDO signatures in the Atlantic or Indian Ocean SST and SLP fields.

Shown in Fig. 2b are the SST and SLP fields regressed upon the CTI, thus this map shows anomalies typically associated with a unit standard deviation ENSO index. Comparing Fig. 2a with Fig. 2b, it is evident that the tropical PDO-spatial signatures are in many ways reminiscent of canonical warm-phase ENSO SST and SLP anomalies (Rasmusson and Carpenter 1982). However, the PDO amplitudes in the tropical fields are weaker than those obtained by regressing the surface fields upon the CTI. Likewise, the PDO-regression amplitudes in the Northern Hemisphere extratropics are stronger than those obtained from regressions upon the CTI (ZWB).

To establish the significance and consistency of polarity reversals in time—referred to by some authors as regime shifts—FH–HF and Hare (1996) utilized a technique known as intervention analysis (Box and Tiao 1975), which is an extension of Autoregressive Integrated Moving Average (ARIMA) modeling (Box and Jenkins 1976). We applied this analysis to each of the time series shown in Fig. 1. Intervention analy-

sis is essentially a two sample t test that can be applied to autocorrelated data, which is a common feature of environmental time series. While interventions can take many forms, we tested only step interventions. The implicit model, therefore, for each variable is a sequence of abruptly shifting levels, accounting for a significant portion of the total variance, around which occurs residual variability, either random or autocorrelated.¹

¹We followed the standard three-step process in fitting the intervention models. First we identify a model. For all time series, the initial model consisted of five parameters: Three interventions, a lag-1 autoregressive term and a constant. The three interventions (phase reversals) we used were 1925, 1947, and 1977. The timing of the interventions was derived independently in earlier studies by several of the authors in this study (FH–HF; ZWB). In the second step, parameters are estimated for significance. If any parameters are statistically insignificant, the least significant is dropped and the remaining parameters reestimated. This sequence is repeated as necessary. The model is then accepted if the final step, a white noise test for model residuals, is passed.

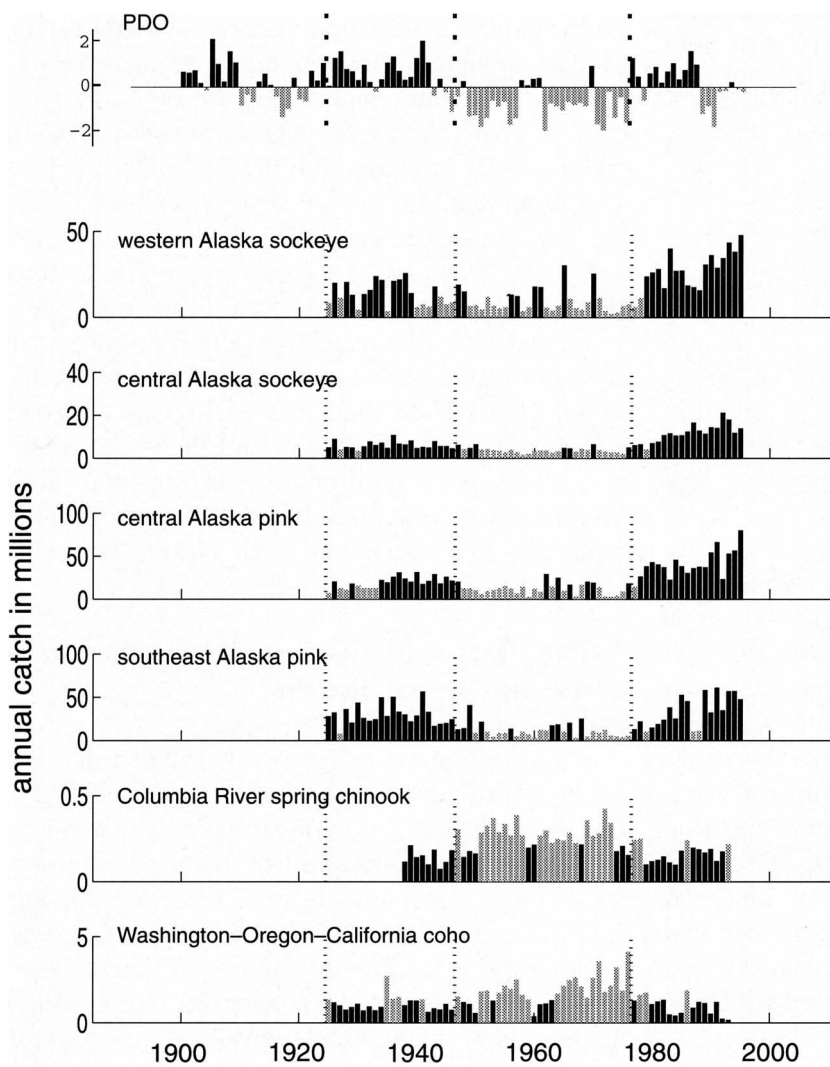


FIG. 6. Selected Pacific salmon catch records with PDO signatures. For Alaska catch, black (gray) bars denote values that are greater (less) than the long-term median. The shading convention is reversed for WOC coho and Columbia River spring chinook catch. Dotted vertical lines are drawn in each panel to mark the PDO polarity reversal times in 1925, 1947, and 1977. At the top, the PDO index is repeated from Fig. 1.

The statistical significance of the intervention model parameters are shown in Table 2. Excluding the CTI, polarity reversals in 1977 are supported in each of the time series shown in Fig. 1. Additional sign reversals in 1925 and 1947 are supported by the PDO and NPPI time series but not for the SOI or CTI.

The implications of this statistical exercise are as follows. We have identified an interdecadal climate signal that is evident in the oceanic and atmospheric climate record. We attribute these signatures to the PDO. During this century, using the North Pacific SST pattern time series as the indicator of polarity, the PDO was predominantly posi-

tive between 1925 and 1946, negative between 1947 and 1976, and positive since 1977. Note that these multidecade epochs contain intervals of up to a few years in length in which the polarity of the PDO is reversed e.g., the positive PDO values in 1958–61, and the strongly negative PDO values in 1989–91).

4. Coastal and continental signatures of the PDO

The signature of the PDO is clearly evident in the wintertime surface climate record for much of North America but not for that of the other continents. The strongest coefficients of wintertime air temperature regressed upon the PDO index are located in northwestern North America (Fig. 3a; cf. Latif and Barnett 1994, Fig. 5b), with local maxima of opposing centers over south central Alaska–western Canada and the southeastern United States. The PDO is positively correlated² with wintertime precipitation along the coast of the central Gulf of Alaska and over northern Mexico and south Florida, and negatively correlated with that over much of the interior of North America and over the Hawaiian Islands.

The continental PDO surface climate signatures are consistent with PDO-related circulation anomalies on the hemispheric scale. The Pacific–North America (PNA) (Wallace and Gutzler 1981) pat-

²To highlight the regional patterns of the PDO Dec–Feb precipitation signal over the North American continent, the correlation map is shown instead of the regression map. The regression coefficients are skewed toward extreme values in the Pacific Northwest and central Gulf of Alaska. Typical precipitation anomalies for a unit standard deviation positive PDO are about +20 to +30 mm for the central Gulf of Alaska, –20 to –30 mm for western Washington state, –40 mm for the Hawaiian Islands, +5 mm over northern Mexico, and –10 mm over the Great Lakes.

TABLE 2. P values for tests of step-changes in the mean level of the Pacific basin climate indices shown in Fig. 1. The four time periods tested for changes in the mean level were 1900–24, 1925–46, 1947–76, 1977–96. P-values greater than 0.05 are labeled “ns” (not significant).

Climate Index	Intercept	1925 step	1947 step	1977 step
PDO	ns	0.001	0.000	0.000
NPPI	0.005	0.001	0.000	0.000
SOI	ns	ns	ns	0.001
CTI	ns	ns	ns	ns

tern emerges when the cold season (November–March) 500-mb height fields are regressed upon the PDO index for the period of record 1951–90 (Fig. 4). This relationship suggests that during epochs in which the PDO is in its positive polarity, coastal central Alaska tends to experience an enhanced cyclonic (counterclockwise) flow of warm, moist air, which is consistent with heavier than normal precipitation. Washington state and British Columbia also tend to be subject to an increased flow of relatively warm humid air, but in their case it is within an area of enhanced anticyclonic circulation that is dynamically unfavorable for heavier than normal precipitation.

In an analysis of springtime (1 April) snowcourse data for the western United States, Cayan (1996) finds that the leading eigenvector of snowpack variability, what he calls the Idaho pattern, is centered in the Pacific Northwest. Cayan's time series for the Idaho pattern has tracked our PDO index since at least 1935 (when his data begins). This pattern of snowpack variability is consistent with the PDO-related wintertime air temperature and precipitation patterns shown in Fig. 3: relatively warm (cool) winter air temperatures and anomalously low (high) precipitation during positive (negative) PDO years contribute to reduced (enhanced) snowpack in the Pacific Northwest. Furthermore, Cayan's composite wintertime 700-mb height fields for the extreme years reveal that variability in the Idaho snowpack pattern is largely controlled by PNA circulation anomalies (cf. Cayan's Figs. 3 and 6 with our Figs. 3b and 4).

We used the PDO correlation and regression maps (Figs. 2 and 3) as guides to search for the local

and regional instrumental records of PDO-driven climate variability shown in Fig. 5. Wintertime surface air temperature along the Gulf of Alaska, and SST near the coast from Alaska to southern California, varies in phase with the PDO. During positive PDO years the annual water year discharge in the Skeena, Fraser, and Columbia Rivers is on average 8%, 8%, and 14% lower, respectively, than that during negative PDO years. In contrast, positive-PDO-year discharge from the Kenai River in the central Gulf of Alaska region is on average about 18% higher than that during the negative polarity PDO years. Cayan and Peterson (1989) also noted that this dipole pattern in west coast streamflow fluctuations is related to the favored pattern of SLP variability in the North Pacific.

5. The PDO and salmon production in the northeast Pacific

Commercial fisheries for Alaskan pink and sockeye salmon are among the most lucrative in the United States (U.S. Department of Commerce 1994, 1995). The unique life history of salmon, which begins and ends in freshwater streams and involves an extensive period of feeding in the ocean pasture, makes them vulnerable to a variety of environmental changes. A growing body of evidence suggests that many populations of Pacific salmon are strongly influenced by marine climate variability (Pearcy 1992; Beamish and Bouillon 1993; FH-HF; Beamish et al. 1995; Francis et al. 1997).

A remarkable characteristic of Alaskan salmon abundance over the past half-century has been the large fluctuations at interdecadal timescales that resemble those of the PDO (Fig. 6, see also Table 3) (FH-HF; Hare 1996). Time series for WOC coho and Columbia River spring chinook landings tend to be out of phase with the PDO index (Fig. 6), though the correspondence is less compelling than that with Alaskan salmon. The weaker connections between the WOC and Columbia River salmon populations and the PDO may be a result of differing environmental–biological interactions. On the other hand, climatic influences on salmon in their southern ranges may also be masked or overwhelmed by anthropogenic impacts: Alaskan stocks are predominantly wild spawners in pristine watersheds, while the WOC coho and Columbia River spring chinook are mostly of hatchery ori-

gin and originate in watersheds that have been significantly altered by human activities.

The best-fit interventions for the Alaskan sockeye stocks occur 2 and 3 yr after those identified in the PDO history, while the best-fit interventions for the Alaskan pink salmon stocks occur 1 yr following the climate shifts (FH–HF). It is believed that sockeye and pink salmon abundances are most significantly impacted by marine climate variability early in the ocean phases of their life cycles (Hare 1996). If this is true, the key biophysical interactions are likely taking place in the nearshore marine and estuarine environments where juvenile salmon are generally found.

Recent work suggests that the marine ecological response to the PDO-related environmental changes starts with phytoplankton and zooplankton at the base of the food chain and works its way up to top-level predators like salmon (Venrick et al. 1987; FH–HF; Roemmich and McGowan 1995; Hare 1996; Brodeur et al. 1996; Francis et al. 1997). This “bottom-up” enhancement of overall productivity appears to be closely related to upper-ocean changes that are characteristic of the positive polarity of the PDO. For example, some phytoplankton–zooplankton population dynamics models are sensitive to specified upper-ocean mixed-layer depths and temperatures. For the decade following the 1960–76 period of record, such models have successfully simulated aspects of the observed increases in Gulf of Alaska productivity as a response to an observed 20%–30% shoaling and 0.5° to 1°C warming of the mixed layer (Polovina et al. 1995).

To the extent that high streamflows favor high survival of juvenile salmon, PDO-related streamflow variations are likely working in concert with

the changes to the near-shore marine environment in regard to impacts on salmon production. For Alaskan salmon, the typical positive PDO year brings enhanced streamflows and nearshore ocean mixed-layer conditions favorable to high biological productivity. Generally speaking, the converse appears to be true for Pacific Northwest salmon.

6. Discussion

Our synthesis of climate and fishery data from the North Pacific sector highlights the existence of a very large-scale, interdecadal, coherent pattern of environmental and biotic changes. It has recently come to our attention that Minobe (1997) has compiled a complementary study of North Pacific climate variability that includes SST indices from the coastal Japan and Indian Ocean–Maritime Continent regions. Especially relevant to our work is the fact that Minobe used instrumental records to independently identify the same dates we promote for climatic regime shifts (1925, 1947, and 1977). Also intriguing is Minobe’s analysis of (tree ring) reconstructed continental surface temperatures that suggest PDO-like climate variability has a characteristic recurrence interval of 50–70 yr and that these fluctuations are evident throughout the past 3 centuries.

It is clear from a visual inspection of the time series shown in Figs. 1, 5, and 6 that not all changes in our PDO index are indicative of interdecadal regime shifts that are equally apparent in the other indices. The difficulties inherent in real-time assessment of the state of the PDO are illustrated by the recent period of record: Alaskan salmon catches and coastal SSTs have remained above average since the late 1970s, while, in contrast, the PDO index dipped well below average from 1989–91 and has hovered around normal since this time. Without the benefit of hindsight it is virtually impossible to characterize such periods and to recognize long-lived regime shifts at the time they occur.

The ENSO and PDO climate patterns are clearly related, both spatially and temporally, to the extent that the PDO may be viewed as ENSO-like interdecadal climate variability (Tanimoto et al. 1993; ZWB). While it may be tempting to interpret interdecadal climatic shifts as responses to individual (tropical) ENSO events, it seems equally

TABLE 3. Percent change in mean catches of four Alaskan salmon stocks following major PDO polarity changes in 1947 and 1977. Mean catch levels were estimated from intervention models fitted to the data and incorporating a 1-yr lag for both pink salmon stocks, a 2-yr lag for western sockeye, and a 3-yr lag for central sockeye.

Salmon stock	1947 step	1977 step
Western AK sockeye	−37.2%	+242.2%
Central AK sockeye	−33.3%	+220.4%
Central AK pink	−38.3%	+251.9%
Southeast AK pink	−64.4%	+208.7%

conceivable that the state of the interdecadal PDO constrains the envelope of interannual ENSO variability.

To our knowledge, there are no documented robust relationships between Pacific salmon abundance and indices of ENSO. The slowly varying time series of salmon catches examined in this study are much more coherent with the interdecadal aspects of the PDO than the higher frequency fluctuations in tropical ENSO indices. In the future it seems very likely that the PDO will continue to change polarity every few decades, as it has over the past century, and with it the abundance of Alaskan salmon and other species sensitive to environmental conditions in the North Pacific and adjacent coastal waters.

This climatic regime–driven model of salmon production has broad implications for fishery management (Hare 1996; Adkison et al. 1996). The most critical implication concerns periods of low productivity, such as currently experienced by WOC salmon. Management goals, such as the current legislative mandate to double Washington State salmon production³ (Salmon 2000 Technical Report 1992), may simply not be attainable when environmental conditions are unfavorable. Conversely, in a period of climatically favored high productivity, managers might be well advised to exercise caution in claiming credit for a situation that may be beyond their control.

Acknowledgments. We thank Ileana Bladé and Nick Bond for carefully reading an early draft of this article and offering constructive critiques. This study was prompted by the University of Washington's interdisciplinary project, "An Integrated Assessment of the Dynamics of Climate Variability, Impacts, and Policy Response Strategies for the Pacific Northwest," and was funded by NOAA's cooperative agreement #NA67RJ0155, Washington Sea Grant, and The Hayes Center.

References

- Adkison, M. D., R. M. Peterman, M. P. Lapointe, D. M. Gillis, and J. Korman, 1996: Alternative models of climatic effects on sockeye salmon (*Oncorhynchus nerka*) productivity in Bristol Bay, Alaska and Fraser River, British Columbia. *Fish. Oceanogr.*, **5**, 137–152.
- ³"The [Washington State] legislature hereby establishes a production goal to double the state-wide salmon catch by the year 2000" (Salmon 2000 Technical Report 1992).
- Alaska Department of Fish and Game (ADFG), 1991: Alaska commercial salmon catches, 1878–1991. Division of Commercial Fish Regional Information Rep. 5J91-16, Juneau, AK, 88 pp. [Available from Alaska Department of Fish and Game, P.O. Box 25526, Juneau, AK 99802.]
- Beamish, R. J., and D. R. Bouillon, 1993: Pacific salmon production trends in relation to climate. *Can. J. Fish. Aquat. Sci.*, **50**, 1002–1016.
- , G. E. Riddell, C.-E. M. Neville, B. L. Thomson, and Z. Zhang, 1995: Declines in chinook salmon catches in the Strait of Georgia in relation to shifts in the marine environment. *Fish. Oceanogr.*, **4**, 243–256.
- Box, G. E. P., and G. C. Tiao, 1975: Intervention analysis with applications to economic and environmental problems. *J. Amer. Stat. Assoc.*, **70**, 70–79.
- , and G. M. Jenkins, 1976: *Time Series Analysis: Forecasting and Control*. Holden-Day, 575 pp.
- Brodeur, R. D., and D. M. Ware, 1992: Interannual and interdecadal changes in zooplankton biomass in the subarctic Pacific Ocean. *Fish. Oceanogr.*, **1**, 32–38.
- , B. W. Frost, S. R. Hare, R. C. Francis, and W. J. Ingraham Jr. 1996: Interannual variations in zooplankton biomass in the Gulf of Alaska and covariation with California Current zooplankton. *Calif. Coop. Oceanic Fish. Invest. Rep.*, **37**, 80–99.
- Cayan, D. R., 1996: Interannual climate variability and snowpack in the western United States. *J. Climate*, **9**, 928–948.
- , and D. H. Peterson, 1989: The influence of the North Pacific atmospheric circulation and streamflow in the west. *Aspects of Climate Variability in the Western Americas, Geophys. Monogr.*, No. 55, Amer. Geophys. Union, 375–397.
- Ebbesmeyer, C. C., C. A. Coomes, C. A. Cannon, and D. E. Bretschneider, 1989: Linkage of ocean and fjord dynamics at decadal period. *Climate Variability on the Eastern Pacific and Western North America, Geophys. Monogr.*, No. 55, Amer. Geophys. Union, 399–417.
- , D. R. Cayan, D. R. McLain, F. H. Nichols, D. H. Peterson, and K. T. Redmond, 1991: 1976 step in the Pacific climate: Forty environmental changes between 1968–1975 and 1977–1985. *Proc. Seventh Annual Pacific Climate Workshop*, Asilomar, CA, California Dept. of Water Research, 115–126.
- Eischeid, J. K., H. F. Diaz, R. S. Bradley, and P. D. Jones, 1991: A comprehensive precipitation data set for global land areas. U.S. Dept. of Energy, Carbon Dioxide Research Program DOE/ER-69017T-H1, TR051, Washington, DC, 81 pp. [Available from CDIAC, Oak Ridge National Laboratory, P.O. Box 2008, Oak Ridge, TN 37831-6335.]
- Fletcher, J. O., R. J. Slutz, and S. D. Woodruff, 1983: Towards a comprehensive ocean–atmosphere dataset. *Trop. Ocean–Atmos. Newslett.*, **20**, 13–14.
- Folland, C. K., and D. E. Parker, 1990: Observed variations of sea surface temperature. *Climate–Ocean Interaction*, M. E. Schlesinger, Ed., Kluwer, 21–52.
- , and —, 1995: Correction of instrumental biases in historical sea surface temperature data. *Quart. J. Roy. Meteor. Soc.*, **121**, 319–367.
- Francis, R. C., and T. H. Sibley, 1991: Climate change and fisheries: What are the real issues? *NW Environ. J.*, **7**, 295–307.
- , and S. R. Hare, 1994: Decadal-scale regime shifts in the large marine ecosystems of the north-east Pacific: A case for historical science. *Fish. Oceanogr.*, **3**, 279–291.

- , —, A. B. Hollowed, and W. S. Wooster, 1997: Effects of interdecadal climate variability on the oceanic ecosystems of the northeast Pacific. *J. Climate*, in press.
- Graham, N. E., 1994: Decadal-scale climate variability in the 1970s and 1980s: Observations and model results. *Climate Dyn.*, **10**, 135–159.
- Hare, S. R., 1996: Low-frequency climate variability and salmon production. Ph.D. thesis, University of Washington, Seattle, 306 pp. [Available from University Microfilms, 1490 Eisenhower Place, P.O. Box 975 Ann Arbor, MI 48106.]
- , and R. C. Francis, 1995: Climate change and salmon production in the Northeast Pacific Ocean. *Can. Spec. Publ. Fish. Aquat. Sci.*, **121**, 357–372.
- Hollowed, A. B., and W. S. Wooster, 1992: Variability of winter ocean conditions and strong year classes of Northeast Pacific groundfish. *ICES Mar. Sci. Symp.*, **195**, 433–444.
- Jones, P. D., and Coauthors, 1985: A grid point temperature data set for the Northern Hemisphere. U.S. Dept. of Energy, Carbon Dioxide Research Division Tech. Rep. TR022, 251 pp. [Available from CDIAC, Oak Ridge National Laboratory, P.O. Box 2008, Oak Ridge, TN 37831-6335.]
- Kushnir, Y., and J. M. Wallace, 1989: Low-frequency variability in the Northern Hemisphere winter: Geographical distribution, structure and timescale. *J. Atmos. Sci.*, **46**, 3122–3142.
- Latif, M., and T. P. Barnett, 1994: Causes of decadal climate variability over the North Pacific and North America. *Science*, **266**, 634–637.
- , and —, 1996: Decadal climate variability over the North Pacific and North America: Dynamics and predictability. *J. Climate*, **9**, 2407–2423.
- Minobe, S., 1997: A 50–70 year climatic oscillation over the North Pacific and North America. *Geophys. Res. Lett.*, **24**, 683–686.
- Namias, J., 1978: Multiple causes of the North American abnormal winter of 1976–77. *Mon. Wea. Rev.*, **106**, 279–295.
- National Fisherman, 1972: August/September 1972. M. Freeman Publications, 88 pp.
- Pacific Fisherman, 1915: September 1915. M. Freeman Publications, 50 pp.
- , 1939: *1939 Yearbook*. M. Freeman Publications, 312 pp.
- Pacific Fishing, 1994: *1994 Yearbook*. Vol. XV, Pacific Fishing Partnership, 116 pp.
- , 1995: *1995 Yearbook*. Vol. XVI, Pacific Fishing Partnership, 90 pp.
- Pearcy, W. G., 1992: *Ocean Ecology of North Pacific Salmonids*. University of Washington Press, 179 pp.
- Polovina, J. J., G. T. Mitchum, and C. T. Evans, 1995: Decadal and basin-scale variation in mixed layer depth and the impact on biological production in the central and North Pacific, 1960–88. *Deep-Sea Res.*, **42**, 1701–1716.
- Rasmussen, E. M., and T. H. Carpenter, 1982: Variations in tropical sea surface temperature and surface wind fields associated with the Southern Oscillation/El Niño. *Mon. Wea. Rev.*, **110**, 354–384.
- Reynolds, R. W., and T. M. Smith, 1995: A high-resolution global sea surface temperature climatology. *J. Climate*, **8**, 1571–1583.
- Roemmich, D., and J. McGowan, 1995: Climatic warming and the decline of zooplankton in the California Current. *Science*, **267**, 1324–1326.
- Salmon 2000 Legislation, 1988: Washington State Senate Bill 6647, Olympia, Washington, 339 pp. [Available from Washington Department of Fisheries and Wildlife, 115 General Administration Bldg., Olympia, WA 98504.]
- Tanimoto, Y., N. Iwasaka, K. Hanawa, and Y. Toba, 1993: Characteristic variations of sea surface temperature with multiple time scales in the North Pacific. *J. Climate*, **6**, 1153–1160.
- Trenberth, K. E., 1990: Recent observed interdecadal climate changes in the Northern Hemisphere. *Bull. Amer. Meteor. Soc.*, **71**, 988–993.
- , and D. A. Paolino Jr., 1980: The Northern Hemisphere sea-level pressure data set: Trends, errors and discontinuities. *Mon. Wea. Rev.*, **108**, 855–872.
- , and J. W. Hurrell, 1994: Decadal atmosphere-ocean variations in the Pacific. *Climate Dyn.*, **9**, 303.
- U.S. Department of Commerce, 1994: Fisheries of the United States. Current Fisheries Statistics Rep. 9400, 113 pp. [Available from Fisheries Statistics Div., (F/RE1), National Marine Fisheries Service, NOAA, 1315 East-West Highway, Silver Spring, MD 20910-3282.]
- , 1995: Current Fisheries of the United States. Current Fisheries Statistics 9400, 126 pp. [Available from Fisheries Statistics Div., (F/RE1), National Marine Fisheries Service, NOAA, 1315 East-West Highway, Silver Spring, MD 20910-3282.]
- Venrick, E. L., and J. A. McGowan, D. R. Cayan, and T. L. Hayward, 1987: Climate and chlorophyll a: Long-term trends in the central North Pacific Ocean. *Science*, **238**, 70–72.
- WDF, and ODFW, 1992: Status report: Columbia River fish runs and fisheries, 1938–91. Washington Dept. of Fisheries and Oregon Dept. of Fish and Wildlife, Portland, Oregon, 224 pp. [Available from Oregon Dept. of Fish and Wildlife, 2501 S.W. First Ave., P.O. Box 59, Portland, OR 97207.]
- Walker, G. T., and E. W. Bliss, 1932: World Weather V, Mem. *Quart. J. Roy. Meteor. Soc.*, **4**, 53–84.
- Wallace, J. M., and D. S. Gutzler, 1981: Teleconnections in the geopotential height field during the Northern Hemisphere winter. *Mon. Wea. Rev.*, **109**, 784–812.
- Ware, D. M., 1995: A century and a half of change in the climate of the NE Pacific. *Fish. Oceanogr.*, **4**, 267–277.
- Zhang, Y., 1996: An observational study of atmosphere-ocean interactions in the Northern Oceans on interannual and interdecadal time-scales. Ph.D. thesis, University of Washington. [Available from University Microfilms, 1490 Eisenhower Place, P.O. Box 975 Ann Arbor, MI 48106.]
- , J. M. Wallace, and D. S. Battisti, 1997: ENSO-like interdecadal variability: 1900–93. *J. Climate*, **10**, 1004–1020.





Weather Information Processing
for the 1996 Olympics
IIPS in the Alaskan Region
IIPS in Europe

Visualization and Human Factors
IIPS at the Forecast Systems Laboratory
NWS Modernization Workshop
U.S. National Systems Workshop
Data Acquisition, Management,
and Dissemination
Hydrologic Forecasting and Services
IIPS on the World Wide Web
Applications of Satellite Technology
Research Information Systems
National Weather Service Tele-
communications Gateway
Technology for the
Classroom

©1996 American
Meteorological Society.
Softbound,
B&W, 578 pp.,
\$60.00 list/
\$35.00 members
(includes
shipping and
handling).

**28 January–
2 February 1996**

Atlanta, Georgia

**American
Meteorological
Society**

**Preprint
Volume**

**12th
International
Conference on
Interactive Information
and Processing Systems**

Please send
prepaid orders to:
Order Department,
American
Meteorological
Society,
45 Beacon St.,
Boston, MA
02108-
3693.